

# Production of high-density Ni-bonded tungsten carbide coatings using an axially fed DC-plasmatron

S. Sharafat<sup>a,\*</sup>, A. Kobayashi<sup>b</sup>, S. Chen<sup>a</sup>, N.M. Ghoniem<sup>a</sup>

<sup>a</sup>Mechanical and Aerospace Engineering Department, University of California Los Angeles, Los Angeles, CA 90095, USA

<sup>b</sup>Joining and Welding Research Institute, Osaka University, Osaka 567, Japan

Received 7 June 1999; accepted in revised form 30 April 2000

## Abstract

Using an axial feed DC-plasmatron, mixtures of fine Ni and WC powder (1–3  $\mu\text{m}$ ) were plasma sprayed onto stainless steel substrates. A series of high-density Ni–WC coatings were produced with uniform distribution of WC particles. The small powder sizes coupled with the axial feed system resulted in high vaporization rates of the Ni and significant decomposition of the WC powders. The high vaporization rate of Ni followed by condensation contributes to the high density of the coatings, while the high WC decomposition rate results in low WC content and low hardness values of the coatings. Based on published data and simple energy balance equations, evaporation of as much as 20% of the Ni powder was estimated, and XRD analysis indicates decomposition of as much as 80% of the WC particles. © 2000 Elsevier Science S.A. All rights reserved.

**Keywords:** Vickers hardness test; Plasma spraying; Nickel; Tungsten carbide

## 1. Introduction

### 1.1. General

Since the mid-1990s, the market share of cemented carbides has surpassed that of high-speed steels (HSS), with tungsten carbide (WC) having 50 % and HSS 45 % of the world market, respectively [1]. Production of bulk WC hardmetals is primarily based on powder metallurgy and is a well-established technology. However, cemented WC coatings produced by plasma spraying has become the subject of considerable research and development [2–8]. Cemented WC coatings find use in areas in which wear is prevalent, and recently they have also been identified as leading candidates for replacement of hard chrome plating [2–4]. Bonded WC

offers several advantages over the chrome plating process, such as, lower costs, improved wear resistance, and reduced environmental hazards. The improved wear resistance of WC-coated components is important, because failure in the coating reduces the fatigue lifetime of the substrate due to crack initiation. Furthermore, WC coatings have demonstrated corrosion resistances that surpass those of chrome plating [2].

Coatings produced by vacuum plasma spraying (VPS) combine good adhesion, low porosity, and low levels of internal oxidation [9], however, very little work has been reported on using a DC plasmatron to produce cemented WC coatings. The main advantages of using DC-plasmas are higher temperatures and lack of internal oxidation. This work reports on the development of a cemented-WC coating produced by using a DC-plasmatron in atmospheric conditions.

### 1.2. Plasma-sprayed WC coatings

Over the past decade, development of cemented WC coatings has been an active field of research with most

\* Corresponding author. UCLA, Mechanical and Aerospace Engineering Department, 48-121 Engineering 4, 420 Westwood Plaza, Mail Code 159710, Los Angeles, CA 90095-1597, USA. Tel.: +1-310-825-8917; fax: +209-821-8979.

E-mail address: sharafat@ucla.edu (S. Sharafat).

of the work centering on using HVOF [2–8] and some with a Detonation Gun (D-Gun) [10]. Slavin et al. [5] formed HVOF WC–Co coatings on substrates and found these coatings to possess excellent adhesion and wear resistances. Ding and Tong [6] investigated the wear behavior and mechanism of HVOF plasma sprayed WC–Co and Cr<sub>2</sub>O<sub>3</sub> coatings in sliding contact with steel, copper, and graphite at room temperature. Their results indicate that both the wear rate and the friction coefficient of WC–Co decrease with an increase of the normal load. They showed that protective layers form because of the temperature rise on contacting surfaces. Tu et al. [7] carried out erosion experiments on coatings of Ni-based alloys with different WC contents. They found that Ni–WC35 (wt.%) possessed the best erosion resistance and microstructure. Steinberg et al. [8] plasma sprayed Ni-coated titanium carbide (TiC) and concluded that the wear-resistance was as good as that of WC–Co coatings under the same experimental conditions.

The use of a Ni binder was compared with Co in deposited WC using a D-Gun [10]. Results of this study revealed a wear mechanism, which involved preferential attack of the binder phase and which led to eventual pullout of carbide particles. It was shown that the Ni-based matrix was more resistant to fine particle attack compared with the Co-matrix. The primary reason was the formation of a hard (W,Cr)<sub>x</sub>C<sub>y</sub>–Ni binder structure. Various authors have compared the properties between Ni- and Co-based bonded WC. They find that the properties are equal if not superior when Ni or a Ni–Fe–Co alloy is used [11,12]. Because the properties of cobalt and nickel are very similar, except for their crystal structure (see Table 1), nickel was chosen as the binder material for this work.

### 1.3. The axial-fed DC-plasmatron

The UCLA Plasma Technology Lab is currently operating two hollow-cathode DC-plasmatrons, which can be used in tandem with a vortex generator capable of running at 300 kW at full power. Arata and Kobayashi [13], at the Institute of Joining and Welding Research at the Osaka University developed the hollow-cathode DC-plasmatron in 1986 and later the vortex generator. Fig. 1 shows a schematic view of the internal-transferred arc hollow-cathode plasmatron. The special feature of this device is the ability to inject powder axially into the plasma beam through a central hole in the cathode.

The axial-feeding scheme supplies extremely fine (< 1 μm) particles along the axis of the plasma plume without distorting the plasma flame. Because the powder-feed gas is introduced into the gun as part of the plasma forming gas, the plasma plume is not cooled by any externally injected gases. Furthermore, the

Table 1  
Selected physical and mechanical properties of Co and Ni

Property	Units	Cobalt	Nickel
<i>Physical</i>			
Atomic number		27	28
Density	(g/cm <sup>3</sup> )	8.92	8.91
Crystal structure		HCP	CCP
Electrical resistivity	(mΩ-cm)	6.34	6.84
Melting point	(°C)	1495	1453
Boiling point	(°C)	2900	2730
Thermal conductivity	(W/mK)	100	91
Thermal expansivity	(10 <sup>-6</sup> /°C)	12.5	13.4
Specific heat	(kJ/mol at 25°C)	24.8	26.1
Heat of vaporization	(kJ/mol)	35	378
Heat of fusion	(kJ/mol)	16.2	17.2
First ionization energy	(kJ/mol)	760.4	737.1
Molar volume	(cm <sup>3</sup> )	6.67	6.59
<i>Mechanical</i>			
Young's modulus	(GPa)	209	200
Shear modulus	(GPa)	75	76
Bulk modulus	(GPa)	180	180
Poisson's ratio		0.31	0.31
Hardness Vickers	(MN/m <sup>2</sup> at 20°C)	1043	638
Hardness Brinell	(MN/m <sup>2</sup> at 20°C)	700	700

powder feed gas entrains almost 100% of the fed powders without any flow distortion to the plasma plume.

The hollow-cathode plasmatron has successfully been applied to produce a variety of unique coatings, such as nitridation of titanium by Ni plasmas [14], forming 10-μm-thick TiN coatings with exposure times of no more than 10 s. More recently, a 10-μm-thick high quality TiN layer was successfully spray deposited using Ti powder in a reactive plasma spray process with nitrogen [15].

## 2. Experimental procedures

### 2.1. Plasma spraying procedures

The test chamber was not evacuated and no shroud or filler gas was used. Argon is used as both the working gas for the plasma and as the carrier gas for the powder. The hollow-cathode DC-plasmatron operating conditions are summarized in Table 2. The powder is fed using a simple in-house developed powder feeder, which is calibrated before each experiment. This powder feeder is based on the fluidized bed concept, without any moving parts. The feed gas enters the powder feeder from the bottom. Portions of the powder are kept suspended in a small chamber by a vibrator and the turbulence of the feed gas. Because feeding rates depend on the fraction of suspended powder, the feed rate varies significantly over long durations (more than 10% drop above 30 s at 20 l/min). The spraying

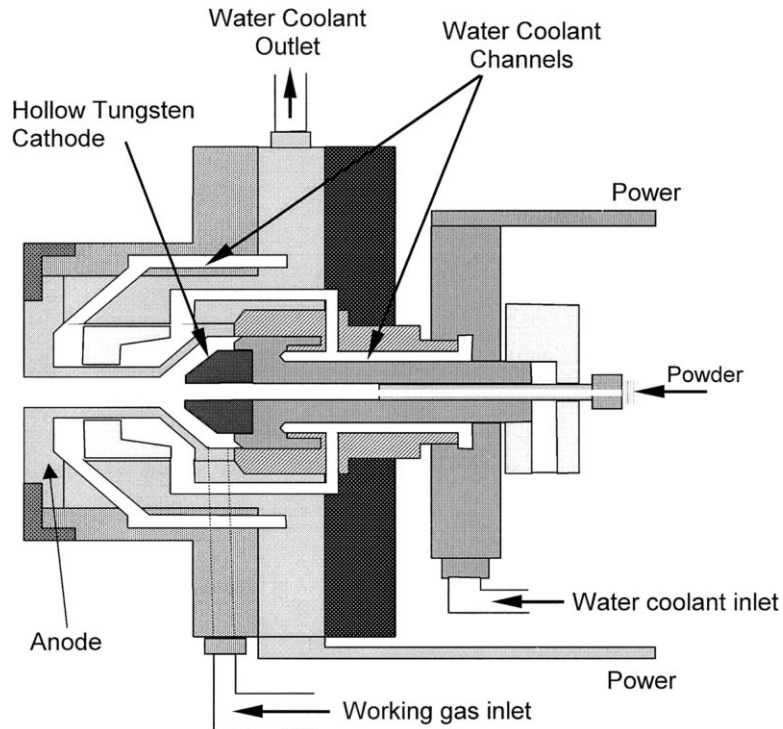


Fig. 1. Schematic of the hollow-cathode DC-plasmatron developed by Arata et al. [13].

durations were limited to below 30 s in order to keep the powder feed rate constant. A commercial powder feeder would significantly increase spraying durations. Build-up of condensation products inside the plasma gun would then be the time limiting factor.

The nozzle to substrate distance was varied between 15 and 30 mm. The substrate coupons are made of 314 stainless steel ( $50 \times 30 \times 3$  mm). They were first mechanically roughened, and then extensively cleaned. The coupons were not actively cooled during spraying.

## 2.2. Test matrix

The test matrix consisted of spraying pure Ni (2–3  $\mu\text{m}$ ), pure WC (1  $\mu\text{m}$ ), and mixtures of these powders. The Ni powder size was chosen in order for the WC and the Ni particles to have similar weights. The WC particles were supplied by PowderMet Inc. and the Ni

particles were purchased from Alfa Aesar [16]. Three different WC/Ni weight ratios were used and based on their WC wt.% are labeled here as WC-25, WC-30, and WC-65. The powders were first dried using electric heaters and then mechanically mixed.

Tables 3 and 4 summarize the test matrix and the operating conditions for each of the powder mixtures. Detailed measurements were performed to establish powder feed rates to the plasma jet. Powder feeding rates ranged between 7 and 15 g/min depending on the powder blend and gas feed rate. During calibration of the powder feeder, it was noted that at a cover gas flow rate of 20 l/min the feed rate for the WC-25 blend was significantly higher than those for the WC-30 or WC-65 (see Table 3). The Ni particles are approximately 2–3 times larger than the WC particles. This results in 4–9 times larger drag forces on the Ni particles compared with the forces on the WC particles. The drag force ( $F_{\text{drag}}$ ) on small particles is primarily a function of particle radius ( $r$ ) and the relative gas velocity ( $v$ ),  $F_{\text{drag}} \propto r^2 v^2$ , and does not depend on the density of the particles. This results in a much larger feed rate of Ni particles relative to the WC, particularly for higher Ni/WC ratios.

## 2.3. Test measurements

Coating thickness and footprint dimensions were recorded. The surface morphology of the coatings was photographed with a magnification of 200 before cutting the coated coupons. The coated coupons were diamond cut through their corresponding maximum

Table 2  
DC-plasmatron operating conditions

	Units	Value
Power	kW	5.3–6.5
Voltage unloaded/loaded	V	75/40
Cooling water flow rate	l/min	8
Working gas	–	Argon
Powder feeder gas	–	Argon
Working gas flow rate	l/min	60
Powder feeder gas flow rate	l/min	15–30
Spraying duration	s	10–20
Substrate distance from nozzle	mm	15–30
Powder feed rate	g/min	7–16

Table 3  
Plasma spray coating conditions

Powder (Ni–WC wt.%)	Carrier gas (l/min)	Powder feed rate (g/min)	Spraying duration (s)	Spraying distance (mm)	Coating thickness ( $\mu\text{m}$ )	Vickers hardness ( $\text{MN}/\text{m}^2$ )
Pure Ni	10	7.2	20	15	200	200
	15	8.2	15	15	180	–
WC-25	15	10.12	15	15	3000	215
	15	7.05	15	15	1550	228
	15	12.78	10	20	1000	235
	15	9.78	10	20	860	–
	–	9.12	10	20	760	–
	15	12.54	10	25	610	–
WC-30	15	15.3	10	30	480	–
	15	2.46	10	15	580	220
	20	6.9	10	15	860	230
	20	9.48	10	20	470	233
WC-65	20	10.62	10	25	1000	–
	20	9.66	10	15	400	230
	–	8	10	20	280	–
	20	10.26	10	20	200	233
Pure WC	25	6.5	10	15	100	300

thickness. They were then potted using an extra low viscosity resin. The samples were polished to a mirror-like finish using 0.25- $\mu\text{m}$  diamond paste. The optical micrographs of the coating cross-sections were taken at magnifications of up to 500. The Vicker's hardness of the pure Ni, WC-25, WC-30, WC-65 (wt.%), and pure WC coatings were measured. X-ray diffraction (XRD) analysis was performed to confirm coating constituents. Both the XRD measurements and the Vickers hardness data substantiate the formation of a Ni-bonded WC coating.

### 3. Experimental results

#### 3.1. Micrographs

Fig. 2 depicts micrographs of the coatings produced using the three Ni–WC mixtures at a magnification of

100. The Ni75–WC25 (wt.%) coating is shown in Fig. 2A and those of Ni70–WC30, and Ni35–WC65 are illustrated in Fig. 2B,C, respectively. All four micrographs were taken near the location of the maximum coating thickness. The coating micrographs show a high-density Ni matrix and almost none of the typical DC-plasma deposited coating morphologies, such as, splats, trapped voids, or partially molten particles.

The micrographs of the three coatings reveal very similar morphologies. The only pronounced difference is the smaller maximum thickness of 400  $\mu\text{m}$  for the Ni35–WC65 (Fig. 2C) coating, relative to the Ni75–WC25 (Fig. 2A) and Ni70–WC30 (Fig. 2B), which had maximum thickness of 1000 and 860  $\mu\text{m}$ , respectively. This indicates that the mixture with a higher WC content resulted in a lower deposition rate.

Fig. 3A,B shows the micrograph of the Ni75–WC25 coating at 200 and 500 magnifications, respectively. The high-density Ni matrix and a relatively uniform dis-

Table 4  
Operating conditions for the coatings depicted in Figs. 2–4

Powder (wt.%)	N-75/WC-25	N-70/WC-30	N-35/WC-65
Figure	2A, 3A,B	2B and 4	2C
Plasma power (kW)	5.6	6.0	5.4
Spraying distance (mm)	20	15	15
Spraying duration (s)	10	10	10
Powder feed rate (g/min)	12.78	6.9	9.66
Carrier flow rate (g/min)	15	20	20
Maximum thickness ( $\mu\text{m}$ )	1000	860	400

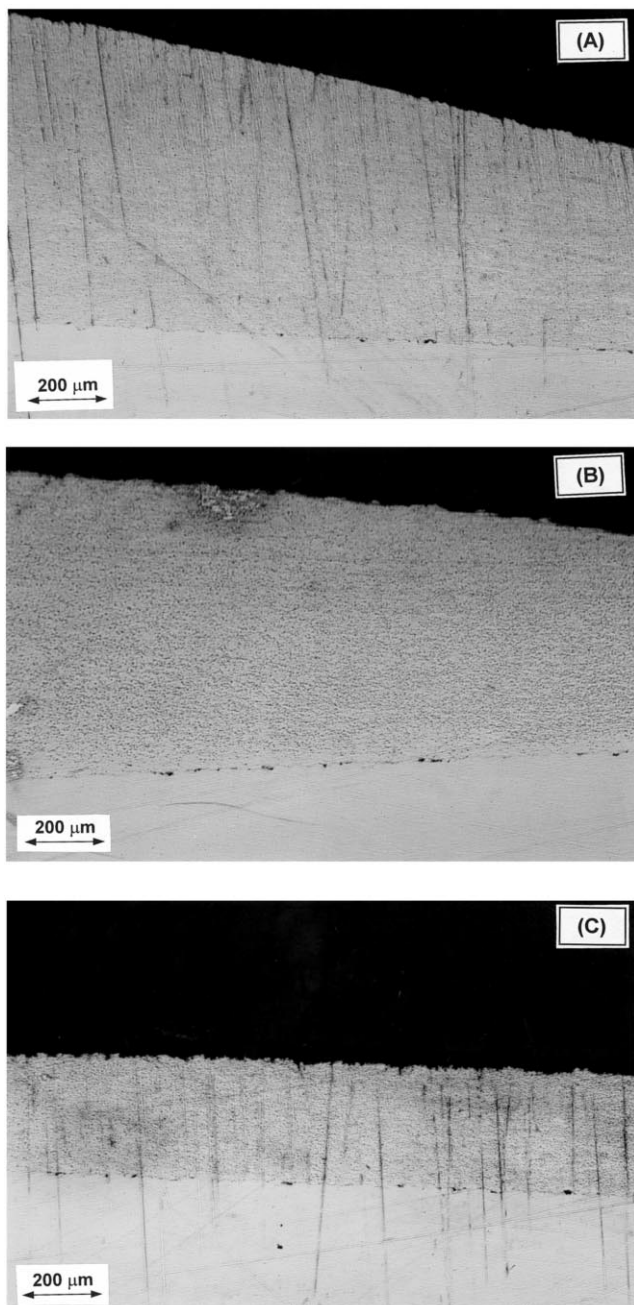


Fig. 2. Micrograph of (wt.%) Ni75–WC25 (A), Ni70–WC30 (B), and Ni35–WC65 (C) coatings.

tribution of the 1- $\mu\text{m}$  WC particles are apparent. The scratch lines across the micrographs are most likely produced by WC particles, which came loose during polishing. This could be indicative of poor bonding of the WC particles, however, we were not able to explain the lack of any scratch-marks for the Ni70–WC30 sample (Fig. 2B). These scratch lines continue into the substrates in a straight line (see Fig. 2A,C), which indicates that they are not a characteristic of the coating itself, such as, cracks.

An even distribution of WC particles was found in

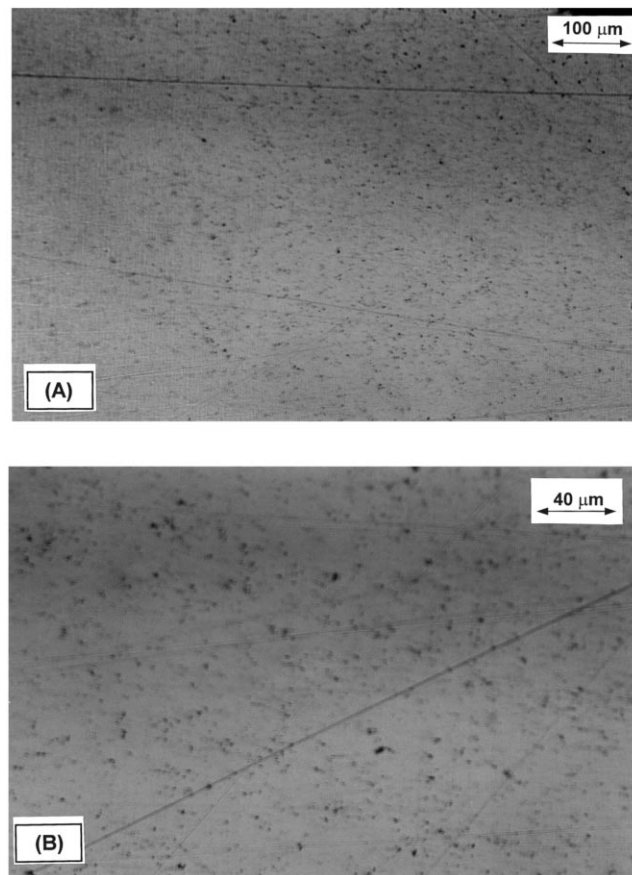


Fig. 3. Micrograph of Ni75–WC25 (wt.%).

the coating made from for the Ni70–WC30 powder mixture (Fig. 4). It is interesting to note that although the WC concentration in the Ni35–WC65 powder mixture is much larger, the micrograph of this high WC loading did not reveal a WC particle density close to that of the Ni30–WC70 coating.

### 3.2. X-Ray diffraction

Fig. 5 shows the results of the XRD analysis of the Ni–WC coatings. Four tungsten phases are identified

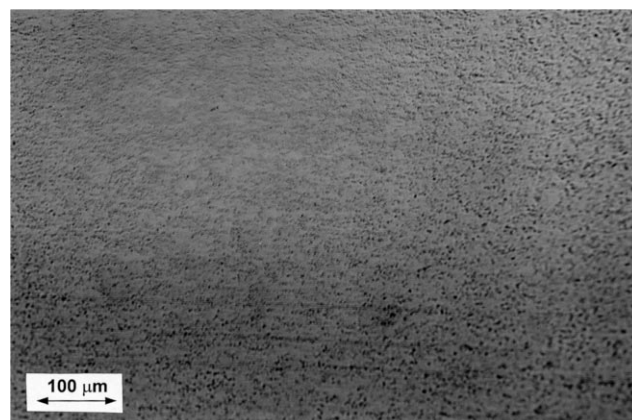


Fig. 4. Micrograph of the Ni70–WC30 (wt.%).

W, WC,  $W_2C$ , and  $WC_{1-x}$ . It is evident that significant levels of decomposition of the WC have occurred. The level of decomposition scales with the WC content of the powder mixture. The 25% WC powder shows little WC decomposition (Fig. 5A), while the 65% WC powder (Fig. 5C) experience significantly higher decomposition levels.

The XRD analysis also shows that the counts for WC do not reflect a one-to-one relationship to the WC weight percent of the powder mixture. Three contributing factors for the reduced WC content in the coatings are discussed in Section 3.5. However, the primary factor is the WC decomposition inside the plasma plume. The powder is introduced into the center of the plasma plume before plasma formation; therefore, the powder traverses the plasma plume during formation

and experiences the longest and hottest in-flight time possible.

Lewis et al. [19] showed that the diffusion of carbon through the WC layer, which forms on the surface of a W particle during carbonization, results in full carbonization of the W particles at an activation energy of 242 kJ/mol between 1056 and 1833°C. It was also reported that the rate of carbonization is inversely proportional to the square of the particle size. Although the activation energy for de-carbonization will be different from that of carbonization, the diffusion of carbon from the inside of a WC particle to a carbon-depleted ( $W_2C$ ) surface would be of the same order and would occur at about the same temperatures. The WC particles used in this experiment are 1  $\mu\text{m}$  in diameter. Based on Lewis's finding, the small size of

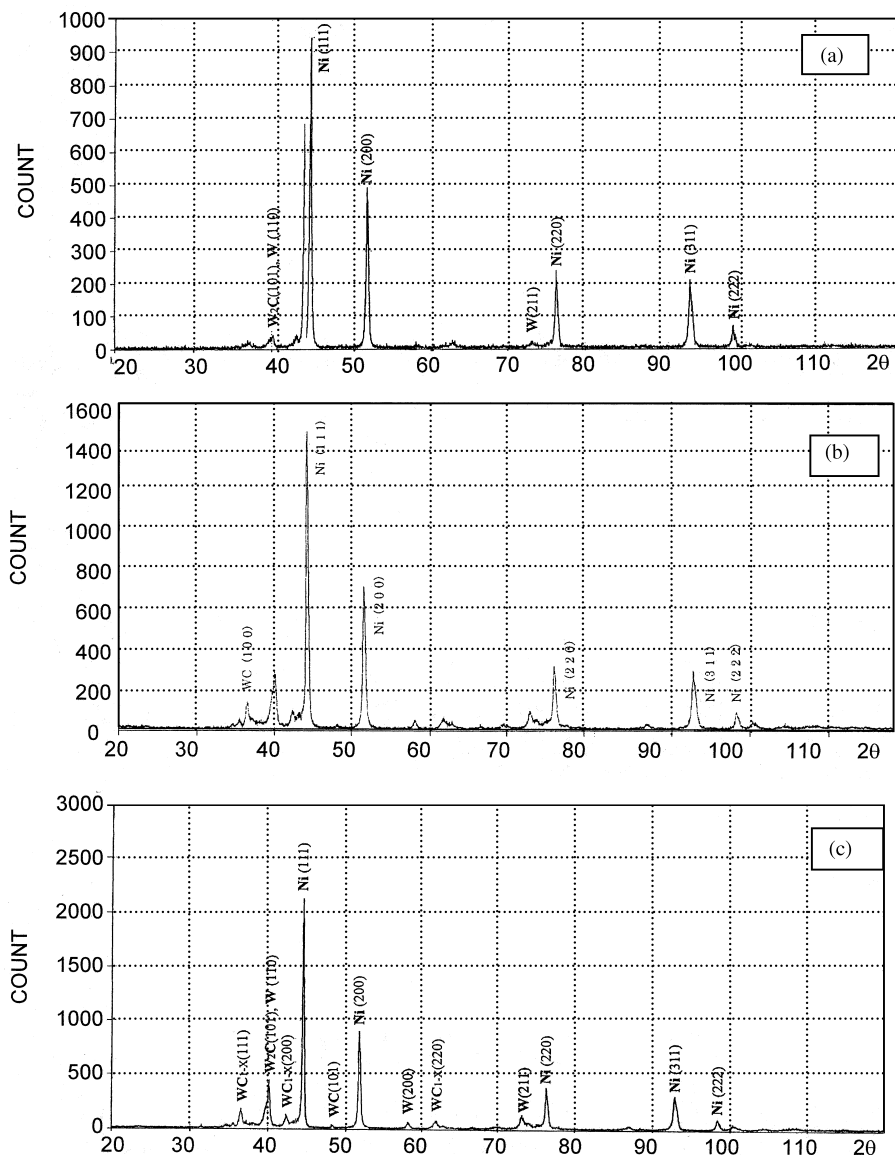


Fig. 5. X-Ray diffraction of (A) Ni75–WC25, (B) Ni70–WC30, and (C) Ni35–WC65 (wt.%) coatings.

these particles should facilitate high decarbonization rates above 2000°C. The change in composition of a WC particle in flight along the axis of the plasma flame is currently being modeled at the UCLA Plasma Technology Lab using non-equilibrium phase transformation and chemical kinetics [20] and will be reported. Furthermore, nickel has been identified to be more prone to the formation of the ‘eta’-phase in the carbon deficient Ni–W–C system, compared with Co [12].

The XRD of the pure WC sample (Fig. 8) shows high levels of pure W deposits. The level of decomposition is estimated to be as high as 80%. This WC coating was produced with a powder feed rate of approximately 6.5 g/min and a power of 5.4 kW (see Table 3). Even at this low power, a WC feed rate of 6.5 g/min is low enough to result in significant decomposition of the ~1- $\mu\text{m}$  WC particles.

### 3.3. Density

The most interesting feature reflected in the micrographs is lack of porosity in the Ni–WC coatings. Based on the XRD and hardness measurements, the high-density coating consists primarily of Ni.

High-density coatings require a high degree of melting and compaction of splats. The gun operates in the subsonic range, which does not result in high splat velocity and therefore compaction is not likely to be the primary cause of the high density. The high density can, however, be explained through a vaporization/condensation model. A simple energy balance approximation was used to estimate a lower bound for Ni evaporation, based on which approximately 20% of the injected Ni powder is fully evaporated during low power (5.5 kW) operation. In case of evaporation, Ni vapor is carried to the target by the plasma plume, where it can condense. This could explain lack of porosity in the high-density coatings shown in Figs. 2 and 3.

Previously published work on depositing Ni substantiates a vaporization/condensation model for low throughputs, which are similar to our conditions. Jahn [17] determined the thermal efficiencies of an axially fed DC-plasmatron from the electrical power input and the heat remaining in the gas after allowing for losses to the cooling water. For operating conditions, similar to those of this work, 60 l/min of Ar at 5 kW power, he resolved the thermal efficiency to be close to 55.7%. In a similar experiment Proulx et al. [18] used a 5-kW inductively coupled DC-plasmatron to deposit pure Ni. The operating conditions were again similar to this work. An argon gas flow rate of 40 l/min was used and the particle feed rate was 10 g/min using 60  $\mu\text{m}$  Ni powder. The present work used approximately 5.5 kW

of power, a gas flow rate of 60 l/min and a powder feed rate of the order of 7–15 g/min with an average powder size between 1 and 3  $\mu\text{m}$ . Proulx found that under those operating conditions, the exit temperature at the center of the plasma jet is approximately 9500 K without any powder. Addition of the Ni powder reduced the flame core temperature to approximately 6000 K at the nozzle exit and to approximately 2500 K at 25 mm away from the exit. It was found that the plasma jet carries enough energy to completely melt the 60- $\mu\text{m}$  Ni particles. The core plasma flame temperature drops much more rapidly for a simple DC-plasmatron compared with an inductively coupled plasmatron. However, in the present work, much smaller sized Ni is directly introduced into the center of the plasma plume and the spraying distance was only approximately 15–20 mm. Assuming a lower thermal efficiency of ~30% and a powder feed rate of 10 g/min an energy balance calculations estimates that approximately 20% of the injected Ni is evaporated if we assign a 1% energy transfer rate from the plasma gas to the powder.

### 3.4. Coating thickness

The coating thickness ranged between 100 and 3000  $\mu\text{m}$  depending on the powder feed rate, Ni/WC ratio, and substrate to plasmatron distance. The operating conditions, which resulted in these thicknesses, are summarized in Table 3. Fig. 6 shows the thickness of coatings as a function of substrate to plasmatron nozzle distance. As the WC content of the powder mixture increases, the coating thickness decreases. The Ni/WC weight ratio affects the thickness because the density of Ni (8.9 g/cm<sup>3</sup>) is approximately 2/3 that of WC (15.7 g/cm<sup>3</sup>). Thus, as the percentage of Ni in the powder mixture increases the coating volume increases, respectively.

### 3.5. Hardness

The Vickers hardness (VH) of the Ni, Ni75–WC25, Ni70–WC30, Ni35–WC65, and pure WC coatings are shown in Fig. 7. The VH of the pure Ni coating was measured to be 200 MN/m<sup>2</sup>, which is approximately one-third the value of the bulk Ni. The coatings of the pure compounds (Ni, WC) were relatively thin and contained significant levels of porosity, which also contributes to low hardness values.

The hardness of the WC–Ni coatings was also found to be low and relatively independent of the WC/Ni ratio. The low hardness measurements can be attributed to a relatively low fraction of WC particles inside the coating. Even with a loading ratio of 65 wt.%

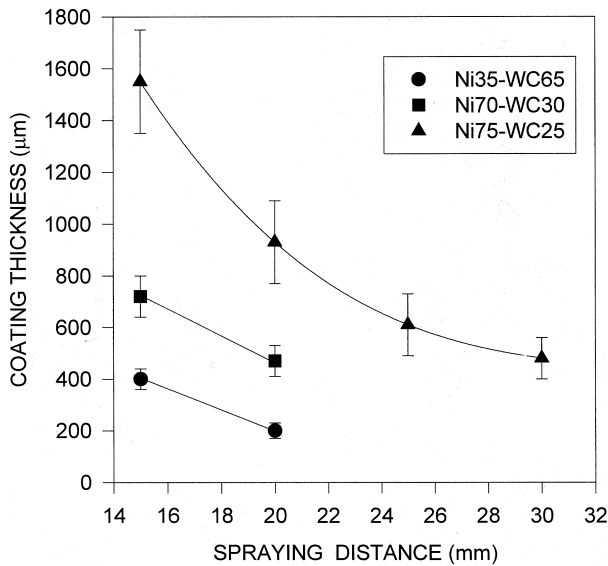


Fig. 6. Maximum coating thickness as a function of spraying distance for three Ni–WC powder mixtures.

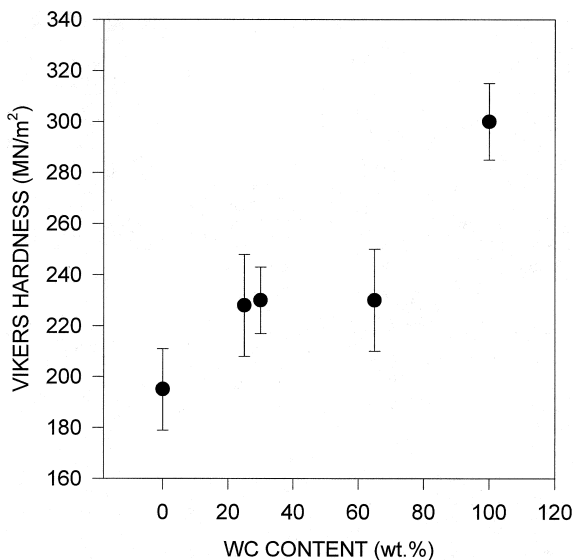


Fig. 7. Vicker's hardness measurements of the cross sectioned coatings for pure Ni, three Ni–WC, and pure WC powder mixtures.

WC, the primary constituent of the powder reaching the gun is Ni, which explains the similarity in density and the hardness values of the coatings produced from different powder mixtures (see Fig. 2). Three potential factors have been identified, which can contribute to a low WC fraction in the coatings:

1. The lower drag force on WC particles relative to Ni results in effectively feeding less WC than present in the powder mixture.
2. The small size of the WC particles (high surface area/volume ratio) enhances the decomposition rate of WC.
3. The powder is fed into the center of the plasma plume before plasma formation, which maximizes the time of flight inside the plasma plume and thereby maximizes heating times.

#### 4. Summary and conclusions

Using an axial feed DC-plasmatron, mixtures of fine Ni and WC powder (1–3 μm) were plasma sprayed onto stainless steel substrates. A series of high-density Ni–WC coatings were produced with uniform distribution of WC particles. However, the small powder sizes coupled with the axial feed system resulted in high vaporization rates of the Ni and in significant decomposition of the WC powders. The high vaporization rate of Ni followed by condensation contributes to the high density of the coatings, while the high WC decomposition rate results in low WC content and low hardness values of the coatings. Based on published data [17,18] and simple energy balance equations, evaporation of as much as 20% of the Ni powder was estimated, and XRD analysis indicates decomposition of as much as 80% of the WC particles.

Three mixtures of Ni and WC powders were deposited at low power (5.5 kW). These mixtures contained WC at 25, 30, and 65 wt.% with the balance

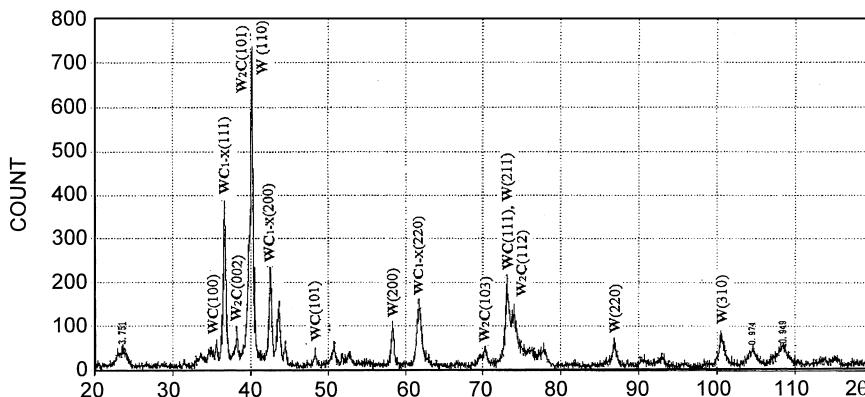


Fig. 8. X-Ray diffraction analysis of a coating using pure 1 μm WC (100 wt.%) powder.

being Ni. The WC powder had an average particle size of 1  $\mu\text{m}$  and the Ni particle size was 2–3  $\mu\text{m}$ . The powder feed rates ranged between 7 and 15 g/min. The 314 stainless steel substrate coupons were positioned between 15 and 25 mm from the plasmatron nozzle. Pure argon was used as both the working gas and the powder carrier gas. The working gas flow rate was 60 l/min and that of the carrier gas was between 15 and 20 l/min. Coating duration times were between 10 and 20 s.

The Ni-based powder mixtures resulted in coating thicknesses of 0.5–3 mm with spraying duration of not more than 20 s. The high-density Ni metal phase exhibited no observable porosity or other geometric features generally associated with DC-plasma sprayed coatings. The interface between the coating and the substrate was also relatively free of pores.

Low hardness values of the Ni–WC coatings indicate low WC loading in the coatings. The coating hardness did not improve significantly with an increase in the WC fraction of the powder mixtures.

X-Ray diffraction measurements showed significant WC decomposition rates Fig. 8. De-carbonization of the WC particle was found to be directly proportional to the WC content of the powder mixture. The maximum decomposition rate of approximately 80% occurred when pure WC powders were plasma sprayed.

#### Acknowledgements

The authors thank PowderMet Inc. for supporting this research. The support of the Joining and Welding Research Institute (Osaka University, Japan) and that of the Ministry of Education (Monbusho, Japan) is also greatly appreciated.

#### References

- [1] G.S. Upadhaya, Cemented Tungsten Carbides, Noyes Publications, Westwood, New Jersey, USA, 1998.
- [2] B.E. Bodger, R.T.R. McGrann, *Plating Surf. Finish.*, September (1997) 28–31.
- [3] T. Seitz, Proc. of the 3rd Global Symposium on HVOF Coatings, Lufthansa AG Report, August 1996.
- [4] R.T.R. McGrann, D.J. Greving, J.R. Shadely, E.F. Rybicki, T.L. Kruecke, B.E. Bodger, *Surf. Coat. Technol.* 108–109 (1998) 59.
- [5] T.P. Slavin, J. Nerz, Proceedings of the Third National Thermal Spray Conference, Metals Park, Ohio ASM International, Long Beach, California, 1990, pp. 159–164.
- [6] C. Ding, Z. Tong. Proceedings of the International Thermal Spray Conference & Exposition, Orlando, Florida, 1992, pp. 673–677.
- [7] J.P. Tu, Z.Y. Mao, L.Z. Wang. Proceedings of the Fourth National Thermal Spray Conference, Pittsburgh, 1991, 53–57.
- [8] T.H. Steinberg, K.J. Niemi. Proceedings of the International Thermal Spray Conference & Exposition, Orlando, Florida, 1992, 661–665.
- [9] D. Matejka, B. Benko, Plasma Spraying of Metallic and Ceramic Materials, John Wiley & Sons, 1989.
- [10] J.K. Knapp, H. Nitta, *Tribol. Int.* 30 (1997) 225.
- [11] A. Gabriel, H. Pastor, D.M. Deo, S. Basu, C.H. Allibert, in: G.C. Kuczynski et al. (Eds.), Sintering 85: World Round Table Conference on Sintering (6th: 1985: Herceg-Novi, Montenegro), New York Plenum Press, 1987.
- [12] H. Suzuki, T. Yamamoto, N.J. Chujo, *Jpn. Soc. Powder Metall.* 14 (1967) 26.
- [13] Y. Arata, A. Kobayashi, Y. Habara, Transactions of the Joining and Welding Research Institute (JWRI), Osaka University, Japan, 15 (1986) 227.
- [14] A. Kobayashi, *Mater. Eng. Perform.* 5 (1996) 373.
- [15] A. Kobayashi, *J. Vacuum*, submitted 1999.
- [16] Alfa Aesar, A Johnson Matthey Co., 1997–98 Catalogue, Ward Hill, MA. 01835-9953, USA.
- [17] R.E. Jahn, *Br. J. Appl. Phys.* 14 (1963) 585.
- [18] P. Proulx, J. Mostaghimi, M. Boulos, *Plasma Chem. Plasma Process.* 7 (1987) 29.
- [19] V.M. Lewis, R. Donelson, R.F. Hehemann, *Metall. Trans. A* 18A (1987) 969.
- [20] M.D. Demetriou, Ph.D. Thesis, Fall 2001.